ESR observation of optically generated solitons in the quasi-one-dimensional iodo-bridged diplatinum complex $Pt_2(n\text{-pentylCS}_2)_4I$

Hisaaki Tanaka,[1] Hideshi Nishiyama,[1] Shin-ichi Kuroda,[1] Takami Yamashita,[2] Minoru Mitsumi,[2] and Koshiro Toriumi[2]
[1]*Department of Applied Physics, Nagoya University, Chikusa-ku, Nagoya 464-8603, Japan*
[2]*Graduate School of Material Science, University of Hyogo, 3-2-1 Kouto, Kamigori-cho, Hyogo 678-1297, Japan*
(Received 22 March 2008; published 9 July 2008)

Light-induced electron spin resonance (LESR) measurements have been performed on a quasi-one-dimensional (Q1D) iodo-bridged diplatinum complex $Pt_2(n\text{-pentylCS}_2)_4I$, where the thermal activation of solitons has been reported in the doubly-degenerate alternate-charge-polarization (ACP) [Pt^{2+}-Pt^{3+}-I^--Pt^{3+}-Pt^{2+}] state formed below 210 K. An enhancement of ESR signal has been detected due to the photogeneration of Pt^{3+} spins below about 30 K, as confirmed through the observed g values of $g_{\parallel}=1.980$ and $g_{\perp}=2.215$ with the external field parallel and perpendicular to the chain axis, respectively. The LESR linewidth is clearly smaller than that of the ESR signal of Curie spins observed under the dark condition, whereas it exhibits uniaxial anisotropy similar to that of the dark ESR due to the anisotropic hyperfine interaction of Pt and iodine nuclear spins. The small LESR linewidth compares well with the motionally-narrowed ESR linewidth of thermally activated solitons at elevated temperatures, indicating that the photogenerated spins are mobile. Furthermore, bimolecular recombination of photogenerated spins has been demonstrated from the excitation power dependence and decay curves of LESR intensity. These LESR features strongly suggest that the mobile spins are photogenerated solitons, which agrees with theoretical predictions.

DOI: 10.1103/PhysRevB.78.033104 PACS number(s): 71.45.Lr, 76.30.He, 71.20.Rv

There has been increasing attention focused on the quasi-one-dimensional (Q1D) halogen (X)-bridged metal (M) complexes, so-called MX-chains, due to their wide variety of physical properties arising from their one-dimensional charge-density wave (CDW) or Mott-Hubbard ground state.[1–4] These electronic states are formed depending on the relative magnitude of electron-phonon interaction (S) to on-site Coulomb interaction (U), i.e., CDW state [$\cdots M^{2+}\cdots X^-$-M^{4+}-$X^-\cdots$] (M=Pt,Pd) for $S>U$ and Mott-Hubbard state [-M^{3+}-X^--] (M=Ni) for $S<U$.[2–6] Here, dotted ($\cdots$) and solid (-) lines in the CDW state represent the longer and shorter metal-halogen bonds, respectively.

In recent years, more sophisticated MMX-chain complexes have been attracting much interest.[7–9] In these complexes, direct metal-metal bonding creates various kinds of valence ordering patterns, typically represented as: (a) averaged-valence (AV) state [-$M^{2.5+}$-$M^{2.5+}$-X^--$M^{2.5+}$-$M^{2.5+}$-X^--], (b) CDW state [$\cdots M^{2+}$-$M^{2+}\cdots X^-$-M^{3+}-M^{3+}-$X^-\cdots$], (c) charge-polarization (CP) state [$\cdots M^{2+}$-M^{3+}-$X^-\cdots M^{2+}$-M^{3+}-$X^-\cdots$], and (d) alternate-charge-polarization (ACP) state [$\cdots M^{2+}$-M^{3+}-X^--M^{3+}-$M^{2+}\cdots X^-\cdots$]. Here, AV and CP states have finite spin densities on the chain with unpaired electrons on the M^{3+} ions whereas CDW and ACP states are doubly-degenerate nonmagnetic states. The AV state is expected to become metallic when the Coulomb repulsion is weak. In fact, Kitagawa *et al.* have reported that an iodo-bridged diplatinum complex $Pt_2(RCS_2)_4I$ (R=CH_3) exhibits the metallic transport properties above room temperature for the first time among the MX- and MMX-chain complexes.[9] More recently, Mitsumi *et al.* have successfully synthesized a series of $Pt_2(RCS_2)_4I$ ($R=C_mH_{2m+1}$; $m=2-5$) with the strategy of tuning the interchain interactions by employing various alkyl chain (R) lengths of the ligand molecule.[10,11] In these systems, a phase transition between the high-temperature AV state and the low-temperature ACP state has been commonly observed at transition temperatures depending on the length of R.[10–13] In the case of the title complex $Pt_2(n\text{-pentylCS}_2)_4I$, the transition takes place at 210 K.

Electron spin resonance (ESR) spectroscopy is a powerful tool in determining the electronic states of the MX-[3,14,15] and MMX-chain[16] complexes because of its high sensitivity to detect the magnetic M^{3+} ions ($S=1/2$). The phase transitions in $Pt_2(RCS_2)_4I$ have been well demonstrated by our previous ESR measurements for $R=n$-butyl and n-pentyl cases.[17,18] In each complex, a drastic change of the ESR spectra has been observed, accompanied with a significant drop of the spin susceptibility at the transition temperature from the magnetic AV state to the nonmagnetic ACP state. The ESR signals in the AV state are ascribed to the conduction electrons, while those in the nonmagnetic ACP state to the Curie spins presumably associated with the defect sites such as chain ends. The observed g values in the AV and ACP states, however, have shown common values of $g_{\parallel}=1.980$ and $g_{\perp}=2.215$ with the external field parallel and perpendicular to the chain axis, respectively, which confirms that the ESR signals originate from Pt^{3+} ions in both phases.

A pronounced feature in n-pentyl case is the observation of thermally activated solitons in the ACP sate, which is the first experimental detection of solitons among the MMX-chain complexes.[17,18] We have observed a spin concentration enhancement from the Curie law above 20 K owing to the thermal activation of isolated Pt^{3+} states. Moreover, ESR linewidth becomes smaller as the temperature is raised, involving a change of the line shape from nearly Gaussian to Lorentzian. The results are consistent with the motional narrowing of the ESR signal, indicating that the thermally excited spins are mobile. The origin of this mobile Pt^{3+} spin can be ascribed to a soliton kink between doubly-degenerate valence ordering of the ACP state,

that is, $[\cdots Pt^{2+}\text{-}Pt^{3+}\text{-}I^{-}\text{-}Pt^{3+}\text{-}Pt^{2+}\cdots I^{-}\cdots]$ and $[\text{-}Pt^{3+}\text{-}Pt^{2+}\cdots I^{-}\cdots Pt^{2+}\text{-}Pt^{3+}\text{-}I^{-}\text{-}]$, as predicted by theoretical studies.[19–21] In contrast to the observation of thermally activated solitons, however, experimental detection of photogenerated solitons has not been reported yet in the *MMX*-chain complexes despite of the theoretical expectations.

In this Brief Report, we report the direct observation of the photogenerated solitons in $Pt_2(n\text{-pentylCS}_2)_4I$ by using light-induced electron spin resonance (LESR) technique. We have successfully observed photoinduced changes of the ESR signal at 4 K, an enhancement owing to the photogeneration of the Pt^{3+} spins. At the same time, a reduction of ESR signals under the dark condition has also been observed, which can be ascribed to the formation of spin singlet states between the photogenerated spins and pre-existing Curie spins, as explained later. The linewidth of the enhanced LESR component exhibits a uniaxial anisotropy as that of the dark signal owing to the hyperfine (hf) and superhyperfine (shf) interactions of $^{195}Pt(I=1/2)$ and $^{127}I(I=5/2)$ nuclei,[17,18] whereas the linewidth is much smaller than that of the dark signal. The small anisotropic LESR linewidth compares well with the motionally-narrowed ESR linewidth of thermally activated solitons at elevated temperatures, indicating that the photogenerated spins are mobile. Moreover, excitation power dependence and decay curves of the LESR intensity have demonstrated the bimolecular recombination of these spins. These LESR features strongly suggest that the photogenerated Pt^{3+} spins are mobile solitons.

Samples of $Pt_2(n\text{-pentylCS}_2)_4I$ were prepared by the same methods as described elsewhere.[11] ESR measurements were performed by using a Bruker EMX spectrometer at the *X* band. An Oxford ESR-900 gas-flow type cryostat was used for the temperature control. A JASCO SM-5 light source with a 300 W xenon lamp was used to provide excitation of 800 nm by optical fiber delivery. The absolute magnitude of the *g* value was calibrated using diphenylpicrylhydrazyl (DPPH) as a standard. More than 100 single crystalline samples were aligned along their chain axis (*c* axis) on a polyethylene-terephthalate substrate in order to obtain sufficient light-receiving surface. The use of aligned single crystals does not affect the accurate observation of the ESR line shape because the *g* values and spectra show uniaxial anisotropy around the chain axis, or negligible orthorhombicity, in other words, as has been reported in the previous studies.[17,18]

Figure 1(a) shows the first-derivative ESR spectra obtained under the dark (dashed curve) and illumination (solid curve) conditions at 4 K with the external magnetic field *H* perpendicular to the *c* axis. The dark component is ascribed to the Curie spins from temperature dependence study.[17,18] Their concentration is obtained as about 10^{-4} spins per *MMX* unit. The LESR signal is obtained by taking the difference of the ESR signals recorded under the illumination and dark conditions as shown in Fig. 1(b) (upper signal). The LESR signal consists of two components, positive and negative ones as shown by the arrows in Fig. 1(b). The lower signal in Fig. 1(b) is the LESR signal obtained 50 min after turning off the excitation light. The intensity of the positive component decreases remarkably after turning off the excitation light.

Figures 2(a) and 2(b) show the time evolution of the LESR intensity at the peak position of the positive and negative components, respectively. A clear decay of the positive component is observed after turning off the excitation light, whereas the negative component exhibits no recovery to the initial intensity, although the superposed wing of the positive component at the field position of negative signal peak causes a slight deviation of the negative component after turning off the excitation light. This result is consistent with the change of the LESR signal in Fig. 1(b). Such a different decay characteristic indicates that these two components arise from different origins.

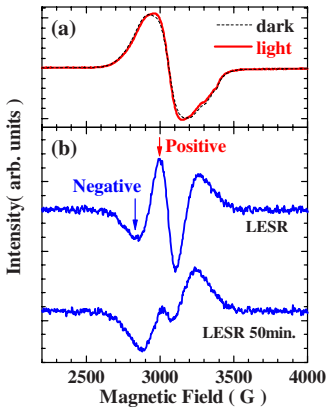

FIG. 1. (Color online) (a) First-derivative ESR spectra obtained under illumination (solid curve) and dark (dashed curve) conditions at 4 K with the external magnetic field *H* perpendicular to the *c* axis. The excitation wavelength is 800 nm and the excitation power is 0.2 m W/cm^2. (b) The LESR signal obtained by taking the difference of the ESR signals recorded under illumination and dark conditions (upper), and that obtained 50 min after turning off the excitation light (lower).

By utilizing the different decay behavior between the positive and negative components, we can extract an approximate line shape of the positive component by taking the difference between the LESR signal recorded under illumination and that recorded 50 min after turning off the excitation light. Figure 3 shows thus obtained LESR signal of the positive component (solid curves) together with the dark ESR signal (dashed curves) for (a) *H* perpendicular and (b) *H* parallel to the *c* axis at 4 K. These signals are normalized by the peak-to-peak intensity. Table I shows the principal *g*

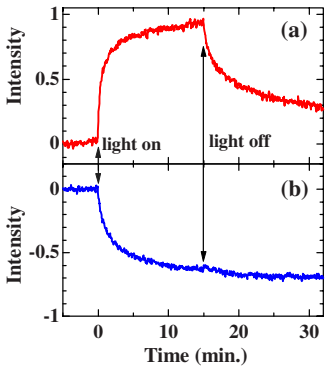

FIG. 2. (Color online) Time evolutions of the LESR intensity at the peak position of (a) the positive component and (b) that of the negative component.

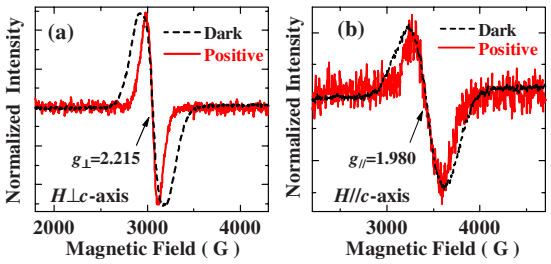

FIG. 3. (Color online) Normalized LESR signal of the positive component (solid curves) for (a) H perpendicular and (b) H parallel to the c axis at 4 K. Corresponding dark ESR signal is also shown by the dashed curve.

values and corresponding peak-to-peak ESR linewidths for both the dark signal and the positive component. The g values of the positive component of $g_\parallel=1.980$ and $g_\perp=2.215$ coincide well with those of the dark ESR, indicating that the positive component arises from the photogenerated Pt^{3+} spins, according to the discussion of the g values of the dark ESR signal reported previously.[17,18]

Next we discuss the motion of the photoinduced spins from the comparison of the anisotropic linewidth of the positive component and that of the dark ESR. In Table I, the uniaxial anisotropy of the linewidth, that is, $\Delta H_{pp\parallel} > \Delta H_{pp\perp}$, is confirmed for both the dark signal and the positive component. This anisotropy reflects that of the hf interactions of Pt and I nuclear spins as discussed previously for the dark signal.[17,18] However, the linewidth of the positive component is clearly smaller than that of the dark signal for both directions, suggesting the occurrence of the motional or exchange narrowing effect. Exchange narrowing, however, is excluded if we consider that the spin concentration of the positive component, comparable to that of the dark spin, is relatively low ($\sim 10^{-4}$ spins per MMX unit). Such low spin concentration is also consistent with the fact that we observe no dipolar broadening of the LESR linewidth even when we increase the spin concentration by employing the higher excitation light power. Then the anisotropy ratio of the linewidth, defined as $\Delta H_{pp\parallel}/\Delta H_{pp\perp}$, further confirms the occurrence of the motional narrowing as in the case of the thermally excited solitons reported in Ref. 18 by the following discussion.

When the motional narrowing takes place with the hopping frequency of ω_e, the resultant linewidth is given as ω_p^2/ω_e under the extreme narrowing condition of $\omega_p \ll \omega_e$. Here, ω_p^2 represents the second moment of the hyperfine-determined linewidth and hence ω_p gives the observed linewidth in the static limit. Thus, the motional effect changes the dependence of the linewidth of ω_p for the static limit to the square dependence of ω_p^2 for the extreme narrowing. Then the ratio $\Delta H_{pp\parallel}/\Delta H_{pp\perp}$ crucially probes the occurrence of motional narrowing by examining whether the anisotropy ratio becomes higher as compared with the static limit value of the Curie spin component of $\Delta H_{pp\parallel}/\Delta H_{pp\perp}=2.0$ observed at 4 K as listed in Table I. The observed value of $\Delta H_{pp\parallel}/\Delta H_{pp\perp}=2.3$ of the positive component in Table I is indeed *higher* than this value, providing strong support for the occurrence of motional narrowing. Furthermore, it is interesting that the above value of the positive component compares considerably well with that of the thermally excited soliton at a higher temperature of 100 K as also shown in Table I.[18] It should be pointed out that not only the ratio but also the absolute value of the linewidth $\Delta H_{pp\perp}$ in both cases also nearly coincide each other. These facts strongly suggest the LESR signals of the positive component are motionally narrowed, indicating the photogeneration of mobile solitons observed for the first time among the *MMX*-chain complexes.

As for the origin of the negative LESR component, its approximate line shape can be obtained by subtracting the positive component from the total LESR signal. The resultant spectral line shape was almost the same as that of the dark ESR signal except for its sign. It should be noteworthy that such negative enhancement of the LESR signal has also been reported in the lightly-doped polythiophene, where the photogenerated polaron ($S=1/2$) couples to the pre-existing polaron created by the chemical doping to form a singlet spin state, that is, spinless bipolaron ($S=0$).[22] In the present system, the negative component may arise from a singlet state between a photogenerated spin and a Curie spin in the dark state formed at defect sites. Thus formed singlet state may be dissociated by thermal energy. In fact, we certainly observed a recovery of the negative LESR component after turning off the excitation light at 50 K, which supports this conjecture. Further discussion of this component is beyond the scope of this work.

Finally, we discuss the recombination kinetics of photogenerated spins, that is, solitons. We observed that the peak intensity of the positive component exhibited $\sim I_{\mathrm{ex}}^{0.5}$ dependence with respect to the excitation power (I_{ex}) up to 0.4 m W/cm^2. This power dependence implies the occurrence of bimolecular recombination (BR) kinetics of the photogenerated spins, which has also been observed for the solitons and polarons in the Pt-I complex of the *MX* chain.[23] In order to demonstrate the BR kinetics more clearly, we com-

TABLE I. Principal g values, ESR linewidths, and linewidth anisotropies obtained for the dark signal and the positive component at 4 K. Those reported for the thermally excited solitons at 100 K are also listed (Ref. 18). The subscripts $\parallel$ and $\perp$ denote the direction of the magnetic field, parallel and perpendicular to the c axis, respectively.

	$g_\parallel$	$g_\perp$	$\Delta H_{pp\parallel}(G)$	$\Delta H_{pp\perp}(G)$	$\Delta H_{pp\parallel}/\Delta H_{pp\perp}$
Dark (4 K)	1.981	2.211	396 ± 10	200	2.0
Positive (4 K)	1.980	2.215	285 ± 10	126	2.3
Thermally excited soliton (100 K)	1.970	2.207	257 ± 10	106	2.4

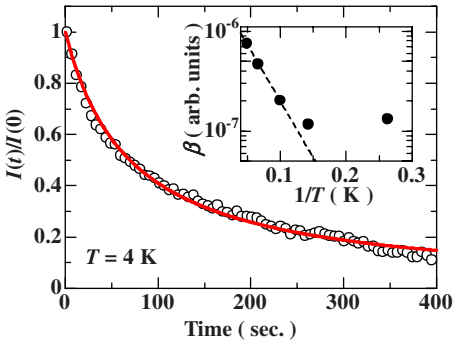

FIG. 4. (Color online) Decay curve of the positive component at 4 K after turning off the excitation light. Duration of the light illumination is 15 min and I_{ex} is 0.4 m W/cm^2. The solid curve is the fitting curves by the BR model. Inset shows the Arrhenius plot of β below 20 K. The dashed line represents the fitting by the activation-type formula.

pare the decay curve of the positive component with that expected for the BR as $I(t)/I(0)=[1+\beta I(0)t]^{-1}$.[23] Here, β is the BR rate constant and $I(t)$ is the LESR intensity, which is proportional to the photogenerated spin number (N), after turning off the excitation light at $t=0$. Figure 4 shows the decay curve of the LESR intensity at the peak position of the positive component at 4 K after turning off the excitation light together with the BR fitting shown by the solid curve. Although we have to add a constant term to the above decay equation in the actual fitting process in order to exclude the superposing negative component, the contribution of which is estimated from the LESR signals shown in Fig. 1(b), BR explains the experimental data considerably well.

Furthermore, the decay curve exhibits clear temperature dependence due to the change of β. The inset of Fig. 4 shows Arrhenius plot of β below 20 K. We find that β obeys activation-type formula of $[\exp(-E_g/k_BT)]$ above 10 K as shown by the dashed line in the figure. Here, E_g is the activation energy and k_B is the Boltzmann constant. Obtained hopping energy is 2.2 meV. Above 20 K, the positive component became hardly observed with sufficient signal-to-noise ratio owing to the rapid recombination of the photogenerated spins. On the other hand, β becomes temperature independent below 10 K. These results indicate that the transport mechanism of the spins exhibits a crossover from high-temperature hopping process to low-temperature quantum tunneling process around 10 K. A similar crossover behavior has been reported in the Pt-I complex of the *MX* chain which is clarified by the photoinduced absorption measurements.[23] However, the pronounced feature of the transport mechanism in the present *MMX*-chain complex is that the magnitude of the activation energy is more than two orders, and the crossover temperature is about an order, smaller than those reported in the *MX*-chain complex.[23] These facts suggest that the mobility of the spins is considerably larger than that in the *MX*-chain complex, which may be qualitatively consistent with the theoretical predictions that much smaller effective mass is expected for the solitons in the *MMX*-chain complexes than those in *MX*-chain complexes.[19]

In summary, the present LESR results for $Pt_2(n\text{-pentylCS}_2)_4I$ provide strong support for the photogeneration of spin soliton in *MMX*-chains predicted by recent theories. As pointed in the case of the thermally exited solitons in the present material,[18] the reversed spin-charge relation[24] and the spatial extent of the solitons would be interesting problems, which are left open for further studies.

This work has been partially supported by a Grant-in-Aid for Scientific Research (Grant Nos. 17740191 and 17340094) and for Science Research in a Priority Area "Super-Hierarchical Structures" (Grant No. 17067007) from the Ministry of Education Culture, Sports, Science and Technology of Japan.

[1] H. Okamoto and M. Yamashita, Bull. Chem. Soc. Jpn. **71**, 2023 (1998), and references therein.
[2] K. Toriumi, Y. Wada, T. Mitani, S. Bandow, M. Yamashita, and Y. Fujii, J. Am. Chem. Soc. **111**, 2341 (1989).
[3] H. Okamoto, K. Toriumi, T. Mitani, and M. Yamashita, Phys. Rev. B **42**, 10381 (1990).
[4] M. Yamashita and S. Takaishi, Bull. Chem. Soc. Jpn. **79**, 1820 (2006).
[5] K. Nasu, J. Phys. Soc. Jpn. **53**, 302 (1984).
[6] K. Iwano, J. Phys. Soc. Jpn. **66**, 1088 (1997).
[7] C. Bellitto, A. Flamini, L. Gastaldi, and L. Scaramuzza, Inorg. Chem. **22**, 444 (1983).
[8] M. Yamashita, S. Takaishi, A. Kobayashi, H. Kitagawa, H. Matsuzaki, and H. Okamoto, Coord. Chem. Rev. **250**, 2335 (2006), and references therein.
[9] H. Kitagawa *et al.*, J. Am. Chem. Soc. **121**, 10068 (1999).
[10] M. Mitsumi *et al.*, J. Am. Chem. Soc. **123**, 11179 (2001).
[11] M. Mitsumi *et al.*, Angew. Chem., Int. Ed. **41**, 2767 (2002).
[12] Y. Wakabayashi, A. Kobayashi, H. Sawa, H. Ohsumi, N. Ikeda, and H. Kitagawa, J. Am. Chem. Soc. **128**, 6676 (2006).
[13] K. Saito *et al.*, J. Phys. Chem. B **109**, 2956 (2005).
[14] K. Marumoto, H. Tanaka, S. Kuroda, T. Manabe, and M. Yamashita, Phys. Rev. B **60**, 7699 (1999).
[15] H. Tanaka, K. Marumoto, S. Kuroda, T. Manabe, and M. Yamashita, J. Phys. Soc. Jpn. **71**, 1370 (2002).
[16] K. Marumoto *et al.*, Solid State Commun. **120**, 101 (2001).
[17] H. Tanaka, S. Kuroda, T. Yamashita, M. Mitsumi, and K. Toriumi, J. Phys. Soc. Jpn. **72**, 2169 (2003).
[18] H. Tanaka, S. I. Kuroda, T. Yamashita, M. Mitsumi, and K. Toriumi, Phys. Rev. B **73**, 245102 (2006).
[19] S. Yamamoto and M. Ichioka, J. Phys. Soc. Jpn. **71**, 189 (2002).
[20] J. Ohara and S. Yamamoto, Phys. Rev. B **73**, 045122 (2006).
[21] M. Kuwabara, K. Yonemitsu, and H. Ohta, in *EPR in the 21st Century*, edited by A. Kawamori, J. Yamaguchi, and H. Ohta (Elsevier, New York, 2002), p. 59.
[22] K. Kaneto and K. Yoshino, Synth. Met. **18**, 133 (1987).
[23] H. Okamoto, Y. Oka, T. Mitani, and M. Yamashita, Phys. Rev. B **55**, 6330 (1997).
[24] A. J. Heeger, S. Kivelson, J. R. Schrieffer, and W.-P. Su, Rev. Mod. Phys. **60**, 781 (1988).